Z. Phys. C – Particles and Fields 33, 135–150 (1986)

Zeitschrift für Physik C Particles and Fields

Probing QCD with Heavy Quarkonia

K. Hagiwara [1] *, A.D. Martin [2], and A.W. Peacock [2]
[1] Deutsches Elektronen-Synchrotron DESY, D-2000 Hamburg, Federal Republic of Germany
[2] Department of Physics, University of Durham, Durham DH1 3LE, UK

Received 11 August 1986

Abstract. The sensitivity of the charmonium and bottomonium spectroscopy to the short distance part of the interquark potential is critically re-examined using the latest data. We confirm that the data cannot accomodate a QCD scale parameter ($\Lambda_{\overline{\rm MS}}$) smaller than about 150 MeV, whereas we find no constraint on larger values for the scale parameter, contrary to a previous analysis. The effect of dynamical heavy quark masses in the loop correction to the perturbative potential is studied in detail and the effective four quark theory with a massive charmed quark is found to give an accurate description of the perturbative potential for quarkonia of mass up to about 200 GeV. It is argued that the experimental determination of the mass and e^+e^- decay width of the $1S$ and $2S$ toponium resonances (of mass round 80 GeV) with the accuracy anticipated at the forthcoming e^+e^- colliders should enable the QCD scale parameter to be determined to within ± 100 MeV.

1. Introduction

Non-relativistic models have been extremely successful in describing the bound states of $c\bar{c}$ and $b\bar{b}$ systems. A variety of flavour independent potentials have been used, ranging from purely phenomenological to QCD-motivated forms with two-loop perturbative contributions at short distances. All these potentials essentially agree in the range $0.1 < r < 1$ fm, which is the interval constrained by $c\bar{c}$ and $b\bar{b}$ quarkonium data [1]. The data do not determine the form of the potential at larger or shorter distances, and so they simply demonstrate the consistency of the QCD form with experiment, rather than prove its existence. On the other hand the much heavier toponium states, when found, probe shorter distance behaviour and have a much better chance of providing direct evidence of the QCD form of the potential, and of determining the QCD scale parameter Λ. To quantify this statement is the main objective of this paper.

Buchmüller and Tye [1] showed that although the ψ and Υ data do not determine the QCD form, they do impose a lower bound on the scale parameter Λ. They conclude $\Lambda_{\overline{\rm MS}} > 0.1$ GeV. The argument is as follows. They assume the next-to-leading order perturbative potential to be reliable in the region $r < r_0$, where $r_0 \Lambda_{\overline{\rm MS}} \sim 0.1$ say. Now if $\Lambda_{\overline{\rm MS}} = 0.1$ GeV the ψ and Υ data are sensitive to the perturbative potential in the region $0.1 \lesssim r \lesssim 0.2$ fm ($\simeq 0.1/\Lambda_{\overline{\rm MS}}$) and reject it, since the slope of the perturbative potential for this value of $\Lambda_{\overline{\rm MS}}$ is less than half that demanded by the data. The Buchmüller-Tye result assumed that the perturbative potential was exact right up to $r = r_0$, where the confining form takes over. The dependence of their result on the lack of smoothness at $r = r_0$ was subsequently studied by Hagiwara et al. [2]. They obtained a smooth potential by introducing a sufficiently flexible form which contributes mainly in the intermediate region $r \sim r_0$ and so does not disturb the short-distance asymptotic behaviour, but which allows small deviations in the region $r \lesssim r_0$ (which can be attributed to higher-order corrections). In practice this is achieved by fitting the parametric form of the overall potential to the perturbative contribution in the interval $r < r_0$ as well as to the ψ and Υ data. The overall potential is constrained by the ψ and Υ data for $0.1 < r < 1$ fm and by the perturbative form for $r < 0.1/\Lambda_{\overline{\rm MS}}$. They concluded $\Lambda_{\overline{\rm MS}} \gtrsim 0.15$ GeV. The analysis led to an upper-bound as well, $\Lambda_{\overline{\rm MS}} \lesssim 0.4$ GeV.

Summarizing the above observations, it is possible to achieve a good description of the ψ and Υ data independent of the value of $\Lambda_{\overline{\rm MS}}$. The sensitivity to $\Lambda_{\overline{\rm MS}}$ only arises if we require the potential to approximate to the perturbative contribution in the short-

* Present address: KEK, Tsukuba, Ibaraki, 305 Japan

distance region where we believe QCD perturbation theory to be valid. For example the description of the data in [3] uses a value of $\Lambda_{\overline{\rm MS}}$ as low as 70 MeV, but at the expense of adding extra sizeable contributions to the perturbative potential throughout the short-distance region.

The purpose of this paper is to critically re-examine charmonium and bottomonium spectroscopy and, in particular, to quantitatively determine the constraints on the QCD scale parameter arising from (i) existing data and (ii) toponium (θ) data when it is available. To do this we use the flexible potential form of [2] to fit to the ψ and Υ data for various fixed values of $\Lambda_{\overline{\rm MS}}$. To examine possible constraints on the value of $\Lambda_{\overline{\rm MS}}$ we compare the potential in the short distance region to the next-to-leading order perturbative contribution. Apart from the existence of a lower bound $\Lambda_{\overline{\rm MS}} \gtrsim 0.15$ GeV we find little sensitivity to the value of $\Lambda_{\overline{\rm MS}}$. This conclusion is unaltered by omitting the charmonium data from the fit.

It is well known [1–7] that toponium spectroscopy is more sensitive to $\Lambda_{\overline{\rm MS}}$.* Phenomenological potentials with different $\Lambda_{\overline{\rm MS}}$, which reproduce ψ and Υ spectroscopy equally well, predict very different results for the heavier θ spectroscopy. The mass difference and the leptonic widths of the $1S$ and $2S$ toponium states will be most accurately measured and are at the same time most dependent on the short-distance properties of the potential. We examine how well the scale parameter $\Lambda_{\overline{\rm MS}}$ can be determined from toponium states produced in e^+e^- experiments with reasonable statistics. We also study the effect of omitting the ψ data from the analysis. This is desirable to avoid the possibility of relativistic corrections affecting the determination of $\Lambda_{\overline{\rm MS}}$.

The structure of the paper is as follows. In Sect. 2 we discuss the details of the next-to-leading order perturbative QCD potential that we use in our analysis, and examine the effect of heavy quark loops (m_c, $m_b \neq 0$). Section 3 describes how we incorporate the long-distance and intermediate contributions into the potential in such a way that $\Lambda_{\overline{\rm MS}}$ is constrained only by the short-distance behaviour of the perturbative contribution to the potential. The results of confronting this potential to the ψ and Υ data are discussed in Sect. 4. We examine the sensitivity of the analysis to the value of $\Lambda_{\overline{\rm MS}}$, and compare the short-distance behaviour of the potential to that of several other potentials which have been used to describe ψ and Υ data. Section 5 describes the accuracy to which experimental information on toponium will be able to determine $\Lambda_{\overline{\rm MS}}$ and section 6 contains our conclusions.

* Igi and Ono [7] have recently performed a very similar analysis to one made in [2]. The authors of [7] are apparently unaware of the previous work [2]

2. The Perturbative Potentials

Our objective is to study the constraints imposed on the QCD perturbative potential by heavy quarkonium data. We must therefore critically review the short-distance static potential between a colour-singlet pair of colour-triplet sources, calculated at the next-to-leading order in QCD perturbation theory, and examine the region of its validity. First, in sub-section *a*, we discuss the perturbative potential in massless QCD and estimate the errors that may arise from higher-order corrections. Then, in sub-section *b*, we study the effects of massive quark loops.

2.a Perturbative Potential in the Next-to-leading Order of Massless QCD

The QCD perturbation expansion for the static potential [8] should be valid at small enough interquark separation since, due to asymptotic freedom [9], the effective coupling constant decreases with decreasing separation, r. The finite part of the one-loop contribution to the static potential has been calculated by several groups [10] in pure gauge theories and by Billoire [11] including the massless quark loop contribution. For n_f massless quarks, the potential can be expressed as

$$V(r) = -\pi C_F \frac{a}{r}[1 + a(b_0 \ln \mu r + A) + O(a^2)] \tag{2.1}$$

with

$$a \equiv \alpha_s(\mu)_{\overline{\rm MS}}/\pi, \tag{2.2}$$

$$b_0 = \tfrac{11}{6} C_A - \tfrac{2}{3} n_f T_F, \tag{2.3}$$

$$A = b_0 \gamma_E + \tfrac{31}{37} C_A - \tfrac{5}{9} n_f T_F. \tag{2.4}$$

Here $\gamma_E = 0.5772$ is the Euler constant, and $T_F = 1/2$, $C_F = 4/3$ and $C_A = 3$ are colour factors. The coupling, α_s, is renormalized in the modified minimal subtraction ($\overline{\rm MS}$) scheme [12] and the unit of mass μ is the scale introduced in the dimensional regularisation.

The coupling satisfies the renormalisation group (RG) equation

$$\mu \frac{\partial a}{\partial \mu} = -a^2[b_0 + b_1 a + O(a^2)] \tag{2.5}$$

with

$$b_1 = \tfrac{17}{12} C_A^2 - \tfrac{5}{6} C_A n_f T_F - \tfrac{1}{2} C_F n_f T_F \tag{2.6}$$

which, neglecting the $O(a^2)$ term, has the solution

$$\Lambda_{\overline{\rm MS}}^{(n_f)} = \mu \exp\left\{-\frac{1}{b_0 a} + \frac{b_1}{b_0^2} \ln\left[\frac{2}{b_0}\left(\frac{1}{a} + \frac{b_1}{b_0}\right)\right]\right\}. \tag{2.7}$$

This equation defines the μ-independent QCD scale parameter $\Lambda_{\overline{\rm MS}}^{(n_f)}$.

We have thus specified the perturbative potential, (2.1), in terms of the constant $\Lambda_{\overline{\rm MS}}^{(n_f)}$. However, before confronting this potential to data two crucial questions must be addressed: up to what distance r and with what accuracy is the truncated expansion, (2.1), valid? Clearly to make a meaningful determination of Λ we need quantitative answers to these questions. This is intimately related to the problem of choosing a good renormalization scale.*

Here we adopt the conservative approach taken in [14]. If there is no a priori reason to expect a perturbation expansion,

$$R=a(\mu)^m\left\{1+\sum_{k=1}^{n} C_k(\mu)[Na(\mu)]^k+O(a(\mu)^{n+1})\right\}, \quad (2.8)$$

for a physical quantity to breakdown, we assume that there exists an optimal scale $\mu_{\rm OPT}$ at which the coefficients of the series in Na satisfy

$$|C_k(\mu_{\rm OPT})|<K=O(1) \quad \text{for } k=1,\ldots n. \quad (2.9)$$

Na, with $N=3$ for QCD, is a natural expansion parameter in large N theories [15]. If we know only the first coefficient C_1, then a first guess μ_1 for the optimal scale is [16]

$$C_1(\mu_1)=0. \quad (2.10)$$

The RG invariance of the physical quantity R gives the second (uncalculated) coefficient in terms of the optimal coefficients as

$$C_2(\mu_1)=C_2(\mu_{\rm OPT})-\frac{b_1}{Nb_0}C_1(\mu_{\rm OPT}). \quad (2.11)$$

Our assumption (2.9), together with (2.3) and (2.6) then implies that the fractional error of the estimate,

$$R=a(\mu_1)^m \quad (2.12)$$

is given by

$$\left|\frac{\Delta R}{R}\right|\simeq|C_2(\mu_1)|[Na(\mu_1)]^2<K[Na(\mu_1)]^2. \quad (2.13)$$

The important observation here is that the choice (2.10) does not introduce artificially large corrections so long as there exists an optimal perturbation expression satisfying (2.9). It is straightforward to see that other more sophisticated assumptions [13] lead to estimates which are consistent with ours to within the error given by (2.13).

Applying the above argument to the perturbative potential of (2.1) we have

$$V_P(r)=-C_F\frac{\alpha_s(\mu_1)_{\overline{\rm MS}}}{r} \quad (2.14a)$$

where our first estimate for the optimal scale is

$$\mu_1=\frac{1}{r}\exp(-A/b_0), \quad (2.14b)$$

and the fractional error

$$|\Delta V_P(r)/V_P(r)|<K\left|\frac{N}{\pi}\alpha_s(\mu_1)_{\overline{\rm MS}}\right|^2. \quad (2.15)$$

The factor K is the order of 1 and, lacking more information, we take $K=1$. With the large colour factor ($N^2=9$) already included this choice is rather conservative. The only available perturbation series to three-loops in QCD are those of unphysical quantities; the RG functions in the $\overline{\rm MS}$ scheme [17], an effective charge in a special momentum (MOM) scheme [18] and its β function [19]. In all these perturbation series the factor K is less than unity for moderate values ($\lesssim 10$) of n_f.

The perturbative potential only gives a good approximation to the quarkonium potential for those values of r for which the fractional error, given by (2.15), is small. The fractional error is shown as a function of $r\Lambda_{\overline{\rm MS}}$ (with $n_f=4$) in Fig. 1. Thus, for example, we expect V_P to be within 10% of the true potential for values of r satisfying

$$r\Lambda_{\overline{\rm MS}}^{(4)}\lesssim 0.08. \quad (2.16)$$

Only in this short-distance region can the data impose meaningful constraints on the perturbative potential. An estimate of the magnitude of higher-order corrections is implicit in any confrontation of perturbation theory predictions with experiment, and it is particularly important in the determination of the QCD scale Λ from heavy quarkonium data. On the one hand it is unjustified to rule out values of Λ by requiring the exact onset of the perturbative potential as r is decreased below a certain value. Even at short-distances we must allow for changes in the potential form arising from the possible higher-order correc-

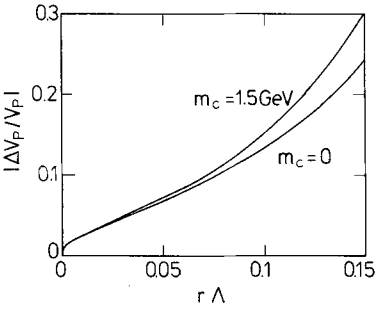

Fig. 1. The fractional error in the perturbative potential (calculated from (2.15) with $K=1$) shown as a function of $r\Lambda$ for $\Lambda\equiv\Lambda_{\overline{\rm MS}}^{(4)}=0.2$ GeV. The plot is essentially the same for other values of Λ. The $m_c=1.5$ GeV curve is calculated using (2.23) in the place of (2.4)

* For a review see, for example, Duke and Roberts [13]

tions. On the other hand we cannot conclude that a certain value of Λ is favoured by a phenomenologically successful potential with the correct $r \to 0$ behaviour, if the potential deviates too much from the perturbative form within its expected region of validity. In order to make an objective, relative judgement for the onset of the perturbative form of the potential we shall make use of the error estimate (2.15) with $K=1$ in the short-distance region specified by the inequality (2.16).

Finally a technical note on the solution of (2.7) for $a \equiv \alpha_s/\pi$ as a function of μ. It is very efficient to solve this equation iteratively as follows [20]

$$a(\mu) \equiv \frac{\alpha_s(\mu)_{\overline{\text{MS}}}}{\pi}$$

$$= \frac{b_0}{b_1} F\left(\frac{b_1}{b_0^2 \ln(\mu/\Lambda_{\overline{\text{MS}}}^{(n_f)}) + b_1 \ln(2b_1/b_0^2)}\right) \tag{2.17a}$$

with

$$F(x) = \lim_{n \to \infty} F^{(n)}(x) \tag{2.17b}$$

where

$$F^{(1)}(x) = x,$$
$$F^{(n)}(x) = [1/x + \ln(1 + 1/F^{(n-1)}(x))]^{-1}$$
$$\text{for } n = 2, 3 \ldots . \tag{2.17c}$$

This iterative solution converges very rapidly at small x.

2.b *Heavy Quark Loop Effects*

It is well known that quark masses can be neglected in loop corrections to the static potential when [21]

$$r^2 m_q^2 \ll 1 \tag{2.18}$$

is satisfied, whereas the effects of heavy quark loops are negligible when [22]

$$r^2 m_q^2 \gg 1. \tag{2.19}$$

Now the $1S$ states of charmonium, bottomonium and toponium ($m_t = 40$ GeV) are sensitive to the potential in the region around $\langle r^2 \rangle^{\frac{1}{2}} = 2.2$, 1.1 and 0.35 GeV^{-1} respectively. Thus toponium (and bottomonium) spectroscopy probe regions where

$$r m_c = O(1) \tag{2.20}$$

and so we must include the effects of massive charmed quark loops. On the other hand from condition (2.19) it appears likely that loop effects due to the bottom quark are negligible. We investigate these effects quantitatively below.

The effect of the charmed quark mass in the perturbative potential was first investigated in [2]. The perturbative potential in massive quark theory has an identical form to (2.1) except that the coefficient A now becomes a function of $m_q r$,

$$A(r) = b_0 \gamma_E + \frac{31}{37} C_A + \frac{2}{3} T_F$$
$$\cdot \sum_{q=1}^{n_f} [\gamma_E + \ln(m_q r) - Ei(-e^{5/6} m_q r)] \tag{2.21a}$$

which gives an excellent approximation to the Fourier transform of the perturbative potential in momentum space. Here $Ei(-x)$ is the exponential integral

$$Ei(-x) = -\int_x^\infty \frac{dt}{t} e^{-t}. \tag{2.21b}$$

For $m_q r \ll 1$ the factor in the square brackets in (2.21a) reduces to $-\frac{5}{6}$, whereas it diverges logarithmically in the $m_q r \gg 1$ limit, signalling the breakdown of infrared decoupling in the $\overline{\text{MS}}$ scheme. This latter problem can be circumvented by using an effective 4-flavour theory [23] provided we stay in the region where the condition

$$r^2 m_b^2 \gg 1 \tag{2.22}$$

is satisfied. Then the coefficient (2.21) becomes

$$A(r) = b_0 \gamma_E + \tfrac{31}{37} C_A + \tfrac{2}{3} T_F [-\tfrac{5}{2} + \gamma_E$$
$$+ \ln(m_c r) - Ei(-e^{5/6} m_c r)] \tag{2.23}$$

where b_0 is given by (2.3) with $n_f = 4$ and where we have set $m_u = m_d = m_s = 0$. The fractional error in the perturbative potential can still be estimated from (2.15), provided the effects of the bottom quark loop are negligible. The result as a function of Λr is also shown in Fig. 1. The error is less than 10% provided

$$r \Lambda_{\overline{\text{MS}}}^{(4)} < 0.07. \tag{2.24}$$

As an example of the sensitivity to the charm quark loop contribution we compare in Fig. 2 the perturbative potential for $\Lambda_{\overline{\text{MS}}}^{(4)} = 0.2$ GeV and $m_c = 1.5$ GeV with that obtained by setting $m_c = 0$. We show only the region probed by the $1S$ toponium state, $0.2 \lesssim r \lesssim 0.5$ GeV^{-1}. We also give the prediction of the effective 3-flavour theory with Λ determined by the matching condition [24]

$$\alpha_s^{(3)}(\mu = m_c) = \alpha_s^{(4)}(\mu = m_c) \tag{2.25}$$

where $\alpha_s^{(n_f)}$ is given by (2.17) with $b_0(n_f)$ and $b_1(n_f)$ given by (2.3) and (2.6). Taking $\Lambda_{\overline{\text{MS}}}^{(4)} = 0.2$ GeV, the matching condition gives $\Lambda_{\overline{\text{MS}}}^{(3)} = 0.25$ GeV. In practice setting $m_c = 0$ does not have a large effect on the toponium predictions. In our example, with $\Lambda_{\overline{\text{MS}}}^{(4)} = 0.2$ GeV the $2S-1S$ energy difference is increased only by 5 MeV on taking $m_c = 0$ rather than 1.5 GeV.

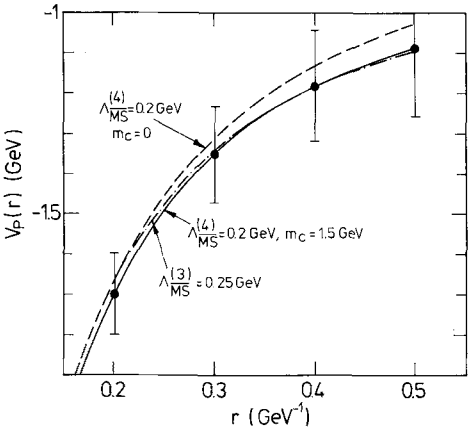

Fig. 2. The behaviour of the perturbative potential for $\Lambda^{(4)}_{\overline{MS}}$ = 0.2 GeV using an expanded scale to show the differences resulting from setting $m_c=0$ and from changing from a $n_f=4$ to a $n_f=3$ effective theory. The errors are calculated using (2.15) with $K=1$

Alternatively, by requiring a given $2S-1S$ mass difference setting $m_c=0$ would decrease the value of $\Lambda^{(4)}_{\overline{MS}}$ by about 20 MeV.

In the rest of this section we study the effects of bottom quark loops quantitatively. The $\overline{MS}$ scheme is not convenient for this purpose because of the presence of the large logarithm in (2.21) in the region $rm_b \gg 1$. Rather, the crossing of the heavy quark threshold is best studied in momentum subtraction (MOM) schemes where the decoupling of heavy quarks is manifest. In such schemes renormalisation and hence the β-function are mass-dependent. Clearly the simplest example of such a coupling constant would be that defined in terms of the static potential [8, 25]

$$\alpha_s(1/r)_V \equiv -rV(r)/C_F \tag{2.26}$$

which, being a physical quantity, has the additional advantage of being gauge invariant. Unfortunately the next-to-leading order coefficient of the corresponding β function, which determines the r dependence of $\alpha_s(1/r)_V$ to the desired accuracy, has not been calculated; this involves two-loop diagrams with massive quarks.

The coefficient is known [26] only for a particular MOM scheme defined at the symmetric Euclidean point of the gluon-ghost-ghost vertex in the Landau gauge. In terms of this coupling constant, which we refer to as $\alpha_s(\mu)_{\mathrm{MOM}}$, the perturbative expansion for the potential has an identical form to (2.1), but with

$$A=A_{\mathrm{MOM}}(r)=A_{\overline{\mathrm{MS}}}(r)-\tfrac{187}{144}C_A+T_F\sum_{q=1}^{n_f}F\left(\frac{m_q^2}{\mu^2}\right) \tag{2.27}$$

where $A_{\overline{\mathrm{MS}}}$ is given by (2.21) with the sum taken over all flavours ($n_f=6$), and where F, the one-loop vacuum polarization function, reads

$$F(x)=-\tfrac{1}{3}\ln x+\tfrac{5}{9}-\tfrac{4}{3}x-\tfrac{1}{3}(1-2x)\,h\ln\left(\frac{h+1}{h-1}\right) \tag{2.28}$$

with $h=(1+4x)^{\frac{1}{2}}$. Noting the limiting behaviour,

$$F(x)=-\tfrac{1}{3}\ln x-\frac{1}{15x}+O(x^{-2}) \quad \text{for } x\gg 1, \tag{2.29a}$$

$$F(x)=\tfrac{5}{9}-2x+O(x^2) \quad \text{for } x\ll 1, \tag{2.29b}$$

we see immediately that the large logarithms (with $m_q r\gg 1$) in $A_{\overline{\mathrm{MS}}}$ and F cancel in (2.27). Indeed from (2.29) we see that heavy quark effects are suppressed by $(m_q r)^{-2}$ in accordance with the decoupling theorem [22]. The optimization of the full theory is carried out just as in (2.14) with the subscript replacement $\overline{\mathrm{MS}}\to\mathrm{MOM}$, where the scale μ_1 is obtained by solving (2.14b) self-consistently since the coefficient A now depends on μ. The scale dependence of the coupling constant $\alpha_s(\mu_1)_{\mathrm{MOM}}$ is governed by the RG equation (2.5) with the coefficients b_0 and b_1 now being quark mass dependent [26], and can hence only be determined by numerical integration. The higher order contribution should still be estimated by (2.15) with the replacement $\overline{\mathrm{MS}}\to\mathrm{MOM}$.

We are now in a position to study quantitatively the region of validity of the effective n_f-flavour theories renormalized in the $\overline{\mathrm{MS}}$ scheme by comparing their predictions with those of the full theory renormalized in the MOM scheme. For illustration we take $\Lambda^{(4)}_{\overline{\mathrm{MS}}}=0.2$ GeV. The trajectories, $\alpha_s^{(n_f)}(\mu)$ versus μ, in the effective n_f-flavour theories are determined by keeping only the first n_f quarks and by fixing $\Lambda_{\overline{\mathrm{MS}}}^{(n_f)}$ through the matching conditions

$$\alpha_s^{(n_f-1)}(\mu=m_f)=\alpha_s^{(n_f)}(\mu=m_f). \tag{2.30}$$

Using $m_{u,d,s}=0$, $m_c=1.5$, $m_b=5$, $m_t=40$ GeV, we find

$$(\Lambda^{(3)}_{\overline{\mathrm{MS}}},\Lambda^{(4)}_{\overline{\mathrm{MS}}},\Lambda^{(5)}_{\overline{\mathrm{MS}}},\Lambda^{(6)}_{\overline{\mathrm{MS}}})=(0.25,0.2,0.13,0.06)\ \mathrm{GeV}. \tag{2.31}$$

To determine the corresponding trajectory, $\alpha_s(\mu)_{\mathrm{MOM}}$ versus μ, in the full theory, we note that for $\mu\gg m_t$ the β functions in the MOM and $\overline{\mathrm{MS}}(n_f=6)$ schemes become identical and that the couplings are related by a shift in the momentum scale [27]

$$\alpha_s(\mu)_{\mathrm{MOM}}=\alpha_s^{(6)}(\mu e^{-t})_{\overline{\mathrm{MS}}} \quad \text{for } \mu\gg m_t \tag{2.32a}$$

with [26]

$$t=(187C_A-80n_f T_F)/[24(11C_A-4n_f T_F)]. \tag{2.32b}$$

All the trajectories, α_s versus μ, are compared in Fig. 3.

We can now determine the perturbative potential for each theory using the optimization procedure of

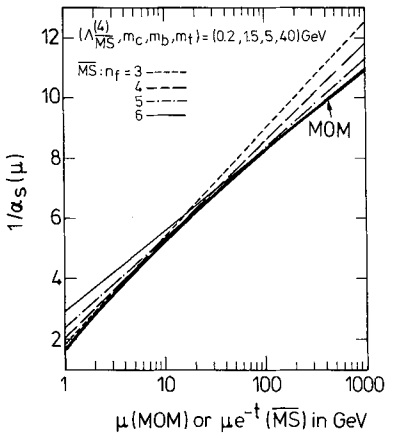

Fig. 3. The trajectories α_s versus μ or $\mu\exp(-t)$ (see (2.32)) for the MOM scheme and the effective n_f-flavour theories in the $\overline{MS}$ scheme. All the curves correspond to taking $(\Lambda^{(4)}_{\overline{MS}}, m_c, m_b, m_t) = (0.2, 1.5, 5, 40)$ GeV

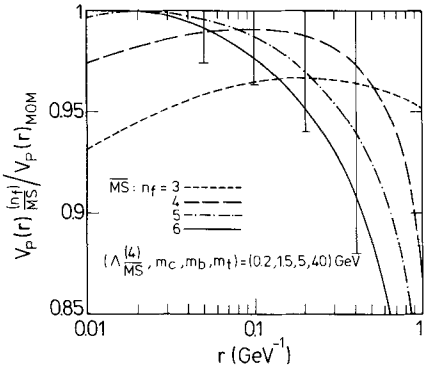

Fig. 4. The perturbative potentials in the effective n_f-flavour theories renormalized in the $\overline{MS}$ scheme normalized to the perturbative potential of the full theory renormalized in the MOM scheme for $(\Lambda^{(4)}_{\overline{MS}}, m_c, m_b, m_t) = (0.2, 1.5, 5, 40)$ GeV. The error bars correspond to (2.15) with $K = 1$

(2.14). The predictions of the effective n_f-flavour theories, normalized to that of the full theory, are shown in Fig. 4. The prediction of the full theory can be best approximated by that of one of the effective n_f-flavour theories, which one depending on the particular region of interest. The small discrepancy of up to 5% is the culumative error arising from higher-order corrections in the RG improvement and in the matching conditions, and is consistent with the error estimate of (2.15) with $K = 1$ as indicated by the error bars. We see from Fig. 4 that the potential calculated in the $n_f = 4$ effective theory, with $\Lambda^{(4)}_{\overline{MS}} = 0.2$ GeV, gives the best approximation to the full theory in the region

$$0.08 \lesssim r \lesssim 0.5 \text{ GeV}^{-1}, \tag{2.33}$$

which includes the entire range in which the perturbative potential can be constrained by heavy quarkonium data. Indeed to start feeling the effects of bottom quark loops we would have to probe the short-distance region $r < 0.08$ GeV^{-1} which would require quarks with $m_q > 250$ GeV. Such quarkonium would instantly decay via weak interactions and cannot be observed [28, 5].

In summary we have critically examined the effect of heavy quark loops in the perturbative potential and found that the effective 4-flavour theory with a massive charm quark gives a good description of the short-distance potential for any forseeable heavy quarkonium phenomenology. We now proceed to investigate whether heavy quarkonia data can determine $\Lambda \equiv \Lambda^{(4)}_{\overline{MS}}$.

3. The Quarkonium Potential

The QCD perturbative potential that we have discussed in Sect. 2 is only valid for small quark separations. In Fig. 5 we show its form in the short-distance region, which we specify by

$$r\Lambda \leqq 0.1, \tag{3.1}$$

for various values of $\Lambda \equiv \Lambda^{(4)}_{\overline{MS}}$. For smaller Λ the perturbative form is valid in a larger region of r. In Sect. 2 we estimated the fractional error due to possible higher-order corrections, and showed it as a function of $r\Lambda$ in Fig. 1. The corresponding errors are indicated on the $\Lambda = 0.2$ GeV potential of Fig. 5. It is important to notice that charmonium and bottomonium data

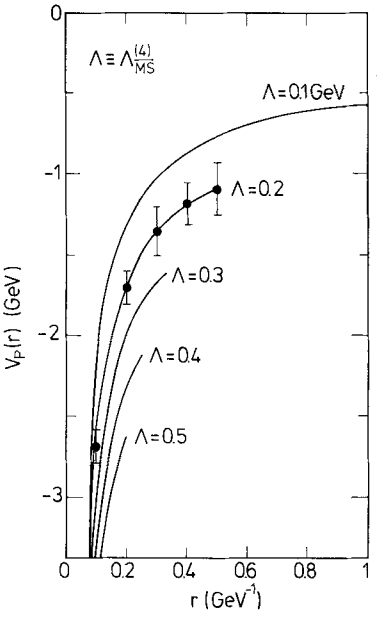

Fig. 5. The perturbative potential $V_P(r)$ for various values of $\Lambda \equiv \Lambda^{(4)}_{\overline{MS}}$ in the region $r\Lambda \leqq 0.1$ where it is expected to be valid. The uncertainty ΔV_P, given by (2.15), is also shown for the $\Lambda = 0.2$ GeV potential

only probe distances greater than 0.5 GeV^{-1} (0.1 fm) and so are only sensitive to values of Λ less than about 0.2 GeV.

We seek a phenomenological potential which embodies the short-distance perturbative behaviour (such that it lies within the perturbative error corridor for $r\Lambda<0.1$) and yet has a sufficiently flexible form so that its behaviour in the $r\Lambda>0.1$ region does not constrain the value of Λ strongly. Both these conditions are crucial for a meaningful determination of Λ.* We follow [2] and use a parametric form

$$V(r)=V_S(r)+V_I(r)+V_L(r) \tag{3.2}$$

where V_S is the short-distance potential to be described below and V_L is the conventional long-range confining potential

$$V_L(r)=ar. \tag{3.3}$$

The "intermediate" component V_I is included solely to give sufficient flexibility at intermediate r values

$$V_I(r)=r(c_1+c_2 r)\exp(-r/r_0) \tag{3.4}$$

and yet to ensure that $V(r)$ approaches the perturbative form at short-distances and also retains long-range linear confinement.

The short-distance component of the potential, V_S, is obtained from the perturbative potential, V_P, by removing the Landau singularity to infinite inter-quark separation. More specifically, the perturbative potential V_P given by (2.14) has a singularity (Landau ghost) at

$$\mu_1=\Lambda\left(\frac{b_0^2}{2b_1}\right)^{b_1/b_0^2}, \tag{3.5}$$

where the next-to-leading order running coupling constant $\alpha_s(\mu)$, as defined by (2.7) or (2.17), blows up. The singularity is clearly seen in V_P shown in Fig. 6 for the case $\Lambda=0.2$ GeV. It occurs at $r\Lambda\simeq 0.3$. The regularized short-distance potential, $V_S(r)$, is then obtained from $V_P(r)$ by shifting the argument of α_s as follows

$$V_S(r)=-\frac{C_F}{r}\alpha_s(\tilde{\mu}_1)_{\overline{\rm MS}} \tag{3.6a}$$

with

$$\tilde{\mu}_1=\mu_1+\Lambda(b_0^2/2b_1)^{b_1/b_0^2}, \tag{3.6b}$$

where the functional form of a $\alpha_s(\mu)_{\overline{\rm MS}}$ is still defined by (2.7) or (2.17). The shift $\mu_1\to\tilde{\mu}_1$ has the effect of removing the singularity to infinite quark separation so that V_S remains finite and approaches zero at large distances (see Fig. 6).

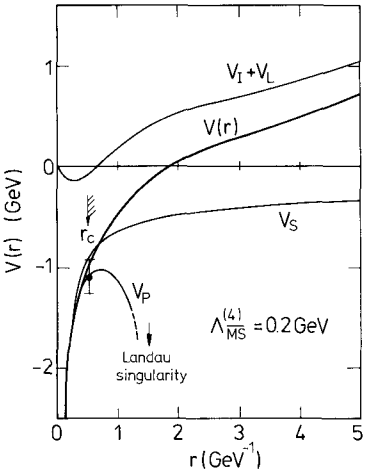

Fig. 6. A typical quarkonium potential, $V(r)$, and its components for $\Lambda=0.2$ GeV: $V(r)=V_S+V_I+V_L$. We require $V(r)$ to lie within an error corridor about the perturbative potential $V_P(r)$in the region $r\leqq r_c$ (with $r_c\Lambda=0.1$). The error defined by (2.15) is shown at $r=r_c$

In summary, all three components of the phenomenological potential (3.2) are regular in the entire interval $0<r<\infty$. $V_S(r)$ dominates at short, and V_L at large, distances, and all three components are important in the intermediate region probed by charmonium and bottomonium spectroscopy. The potential depends on 5 parameters, Λ in V_S, a in V_L and c_1, c_2, r_0 in V_I. These parameters, together with the heavy quark masses* which set the scale of their respective heavy quarkonium spectrum, are to be determined by fitting to the available (and forthcoming) data.

For a meaningful determination of $\Lambda=\Lambda^{(4)}_{\overline{\rm MS}}$ the quarkonium potential $V(r)$ is required to reproduce its perturbative form $V_P(r)$ in the region where the perturbation expansion is expected to be valid, say $r<r_c$. To be specific we define this region by

$$r_c\Lambda=0.1. \tag{3.7}$$

Deviations can occur in this region due to the V_I+V_L component and due to the regularisation of V_P (see Fig. 6). In Sect. 2 we estimated the error $\Delta V_P(r)$ in $V_P(r)$ which may be expected from higher-order corrections. Thus a quantitative measure of the validity of a given phenomenological potential $V(r)$ can, for

* For example the Λ parameter in the phenomenologically successful potential due to Richardson [29] is unrelated to our $\Lambda^{(4)}_{\overline{\rm MS}}$ since its value is determined by the shape of the potential in the intermediate region where the perturbation expansion is not expected to work well

* As discussed in Sect. 2, only the charmed quark mass is needed for the loop corrections to $V_P(r)$. The sensitivity of the spectrum to the actual value used in the loop contribution is found to be very weak and we fix it to be 1.5 GeV independent of the value of m_c determined by the fit to the charmonium data

example, be taken to be

$$\chi_V^2 = \sum_{n=1}^{10} |V(r_n) - V_P(r_n)|^2 / |\Delta V_P(r_n)|^2 \tag{3.8}$$

with $r_n = n r_c/10$. When considering the value of χ_V^2 we should note that it is proportional to K^{-2} and that we have arbitrarily set K of (2.15) equal to unity.

Two final comments about the form of the quarkonium potential are in order. Since we require our potential to have the short-distance perturbative form, we do not allow an overall constant term in the potential. It is known [1, 2] that the major effect of an overall shift in the potential can be compensated for by a change in the quark mass. Since the heavy quark masses (m_c, m_b and m_t) are taken as free parameters, the effect of a constant term can be regarded as a trivial shift of the quark masses. However the constant term V_0 does affect the level spacings and hence we may investigate the effects of adding V_0 to our potential (3.2). For fixed values of Λ we repeated the fits to the quarkonia data including V_0 in our parameter set. Small values of V_0 were preferred. In Sect. 4 we briefly discuss the correlation between the slope, a, of the long-distance part of the potential ($V_L = ar$) and the value of V_0. We also found that the possibility of determining Λ from toponium data is insensitive to the inclusion of V_0.

The second remark concerns a general property of the quarkonium potential. It has been shown [31] that the potential must be a monotonically increasing, concave function of the separation r. That is

$$\frac{dV}{dr} > 0 \quad \text{and} \quad \frac{d^2V}{dr^2} \leqq 0. \tag{3.9}$$

We do not impose these constraints on our parametrization but check, a posteriori, that the potential has this property. We found that the second condition was only occasionally violated slightly and then only in fits to both charmonium and bottomonium data for the smallest values of Λ ($\Lambda \sim 0.1$ GeV) at large values of r ($r \sim 3.5$ GeV^{-1}).

4. Description of Charmonium and Bottomonium Data

Only toponium has a chance of probing the short-distance perturbative behaviour of the potential and we do not expect charmonium or even bottomonium data to put strong constraints on the value of Λ. Rather we use the data to obtain satisfactory phenomenological potentials at various values of Λ with which to confront toponium data when it becomes available. The fine and hyperfine splitting of toponium states are predicted to be of the order of 10 MeV [5] and are beyond the resolution of the presently forseeable experiments. We therefore perform an analysis using the spin-averaged quarkonium levels.

The charmonium and bottomonium data set [32] that we use is shown in Table 1. We do not include the $2S$ charmonium level in the fit due to its proximity to the open flavour threshold and due to mixing effects. The P level is calculated as the spin-averaged centre-of-gravity of the three ^3P_J levels and we neglect possible hyperfine splitting from the unobserved $^1P_1$ level. We take the error to be 10 MeV and keep in mind that the general tendency of hyperfine splitting will cause the true centre-of-gravity to be less than that of the ^3P_J levels. Only the triplet S levels of bottomonium have been observed. The data in Table 1 has been obtained by using the following predictions for the $^3S - {}^1S$ hyperfine splittings:

$$m(\Upsilon) - m(\eta_b) = 32, 16, 11 \text{ MeV}$$

for the $1S$, $2S$, $3S$ levels respectively [33]. Again we take the P levels to be simply the weighted average of the observed three ^3P_J levels. The observed ratios of the leptonic widths are included in the fits by using

$$\frac{\Gamma_{ee}(nS)}{\Gamma_{ee}(1S)} = \left(\frac{m(1S)\, R_{nS}(0)}{m(nS)\, R_{1S}(0)}\right)^2 \tag{4.1}$$

where $R_{nS}(r)$ is the radial wave function. We fit to the ratios rather than to the absolute widths since the latter have large first-order QCD corrections [34]

$$\Gamma_{ee}(nS) = \frac{4\alpha^2 e_q^2}{m(nS)^2} |R_{nS}(0)|^2 \left[1 - \frac{16\alpha_s}{3\pi}\right], \tag{4.2}$$

which are essentially cancelled in the ratios. However, for each fit we present Γ_{ee} calculated from the formula (4.2) by using $\alpha_s(2m_q)_{\overline{\text{MS}}}$.

For various values of $\Lambda \equiv \Lambda_{\overline{\text{MS}}}^{(4)}$ we vary the remaining 4 parameters of the potential (given in Sect. 3) and the external heavy quark masses to obtain the best χ^2 fit to the quarkonia data, simultaneously requiring the potential to approximate to its perturbative short-distance form by including (3.8) in χ^2. As $V(r)$ is varied to achieve the optimum fit we need to repeatedly solve the radial Schrödinger equation. We use the matrix inversion method of [35]. Here the Schrödinger equation is reduced to a matrix equation, using the finite difference approximation for the derivatives, and solved to obtain the eigenvalues and eigenvectors, which correspond to the energy levels and wave functions respectively. The method has been tested for efficiency and accuracy by using a pure Coulombic potential.

In Table 1 the $c\bar{c}$ and $b\bar{b}$ levels are given with respect to the lowest S state. The parameters m_c and m_b ensure that the lowest level is reproduced exactly by the potential.

Table 1. The optimum fits to quarkonia data (and the perturbative potential) for $\Lambda = \Lambda^{(4)}_{\overline{\rm MS}} = 0.2$ and 0.4 GeV. The masses $m(nl)$ are given in MeV and the leptonic widths, $\Gamma_n \equiv \Gamma_{ee}(nS)$, in keV. The data marked by ⋆ are not used in the fit

	Data	$c\bar{c}+b\bar{b}$ data fitted				Only $b\bar{b}$ data fitted			
		$\Lambda=0.2$	χ^2	$\Lambda=0.4$	χ^2	$\Lambda=0.2$	χ^2	$\Lambda=0.4$	χ^2
$c\bar{c}$ data:									
$m(1S)$	3068 ± 2	3068	0	3068	0				
$m(2S)-m(1S)$⋆	595 ± 2	609	–	596	–				
$m(1P)-m(1S)$	457 ± 10	426	9.6	423	11.3				
Γ_2/Γ_1	0.43 ± 0.06	0.49	1.1	0.47	0.3				
Γ_1⋆	4.75 ± 0.51	4.35	–	4.81	–				
$b\bar{b}$ data:									
$m(1S)$	9452 ± 2.5	9452	0	9452	0	9452	0	9452	0
$m(2S)-m(1S)$	567 ± 3	571	1.9	568	0.1	569	0.7	566	0.0
$m(3S)-m(1S)$	900 ± 2.5	902	0.8	903	1.6	902	0.9	902	0.5
$m(1P)-m(1S)$	448 ± 2.5	446	0.8	447	0.3	446	0.3	447	0.1
$m(2P)-m(1S)$	809 ± 6	790	10.3	795	5.4	790	10.4	797	3.1
Γ_2/Γ_1	0.44 ± 0.03	0.39	3.1	0.39	2.4	0.38	3.7	0.39	1.9
Γ_3/Γ_1	0.33 ± 0.03	0.32	0.1	0.31	0.5	0.31	0.2	0.30	1.3
Γ_1⋆	1.22 ± 0.05	1.05	–	1.13	–	1.07	–	1.17	–
$\chi^2_{\rm data}$			27.8		21.9		16.2		6.9
χ^2_V of (3.8)			1.7		1.2		2.4		0.2
Parameter values	m_c (GeV)	1.36		1.58		–		–	
	m_b (GeV)	4.79		4.99		4.82		5.04	
	a (GeV^2)	0.22		0.18		0.21		0.16	
	c_1	−1.12		−1.35		−1.55		−2.54	
	c_2	1.19		1.15		1.40		0.92	
	r_0 (GeV^{-1})	0.70		0.57		0.63		0.36	

We show results as a function of $\Lambda \equiv \Lambda^{(4)}_{\overline{\rm MS}}$ for two series of fits; first fitting to the combined $c\bar{c}$ and $b\bar{b}$ data, and then to the $b\bar{b}$ data alone. The detailed results for $\Lambda = 0.2$ and 0.4 GeV are given in Table 1, whereas in Fig. 7 we show χ^2 as a function of Λ. We see that there is a marked increase in χ^2, particularly in χ^2_V, for $\Lambda \lesssim 0.15$ GeV. This puts on a quantitative footing a result originally given by Buchmüller and Tye [1]; namely low values of Λ are ruled out due to the conflict between the slope of the perturbative potential and the one required by the data in the 0.1–1 fm (0.5–5 GeV^{-1}) region. As Λ increases from 0.15 GeV the experimentally constrained region of the potential separates from the perturbative region and, not surprisingly, we see χ^2_V as defined by (3.8) plays a negligible role in the fit. Apart from the constraint $\Lambda \gtrsim 0.15$ GeV, we conclude that Λ is not determined by $b\bar{b}$ (and $c\bar{c}$) data.⋆

⋆ The rise in χ^2 at larger Λ shown in the fit of [2] is attributable to the inclusion of the observed leptonic width of the $b\bar{b}$ $1S$ state in the fit and in particular to fitting it with (4.2) without the first-order QCD correction

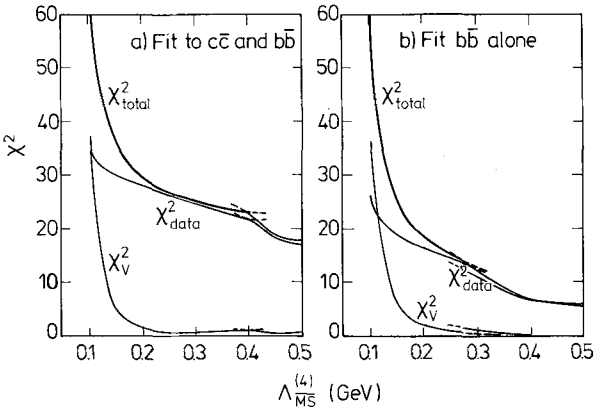

Fig. 7a, b. χ^2 as a function of Λ obtained by fitting **a** the $c\bar{c}$ and $b\bar{b}$ quarkonia data, and **b** the $b\bar{b}$ data alone. The total χ^2 includes a component χ^2_V (given by (3.8)) which is a measure of how well the potential reproduces the perturbative potential in the short-distance region. Note that the optimum solution changes discontinuously from one set of parameters (c_1, c_2, r_0, a, m_q) to another at a certain value of Λ. Including an extra parameter c_3 smooths out the χ^2 profile but does not change its essential character

It is worth stressing that with our flexible intermediate parametrization of the potential we are determining the long-distance confining part of the potential relatively free from its intermediate behaviour. From Table 1 we see that the slope of the linear confining component of the potential ($V_L = ar$) has a value $a \approx 0.2$ GeV^2 essentially independent of the choice of Λ. This value is consistent with that predicted by the string model $a = 1/2\pi\alpha' \simeq 0.17$ GeV^2. This observation is not new; indeed, with the phenomenological potential of the Cornell group [36]

$$V(r) = -\frac{K}{r} + ar \tag{4.3}$$

the best fit ($\chi^2_{\text{data}} = 65.3$) to the combined $c\bar{c}$ and $b\bar{b}$ data has $K = 0.47$ $a = 0.19$ GeV^2, $m_c = 1.32$ GeV and $m_b = 4.75$ GeV. The success of the Buchmüller-Grunberg-Tye potential [1] can also be attributed to its large-distance behaviour being determined by the Regge slope.

We repeated the fits but now including a constant term V_0 in the potential as a free parameter. We found a correlation between V_0 and the slope, a, of the long-distance potential V_L. The results are summarized in Table 2 for $\Lambda = 0.2$ GeV. Acceptable fits are seen to have a slope, a, compatible with that required by string dynamics and a value of V_0 around zero. If, for instance, one chooses a larger value of a ($a > 0.2$ GeV^2) then a negative V_0 is required in an attempt to compensate for the rapid rise of the stored energy as the quark separation increases through the region sensitive to the $c\bar{c}$ and $b\bar{b}$ data.

Finally we briefly consider other phenomenological quarkonium potentials that have been proposed. To obtain a consistent comparison we use each of the potential forms in turn to fit to the $c\bar{c}$ and $b\bar{b}$ data listed in Table 1.

Table 2. The optimum fits to $c\bar{c}$ and $b\bar{b}$ data for $\Lambda = 0.2$ GeV for different fixed values of the slope, a, defined by $V_L = ar$, but with a constant term V_0 included in the potential as a free parameter

a (GeV^2)	V_0 GeV	χ^2
0.35	−0.41	98
0.33	−0.40	74
0.31	−0.35	54
0.29	−0.26	41
0.27	−0.20	34
0.25	−0.10	33
0.23	−0.04	30
0.21	0	29
0.19	0.11	27
0.17	0.19	24
0.15	0.22	46
0.13	0.23	92

(i) Martin Potential [30]. The potential form

$$V(r) = A + Br^v \tag{4.4}$$

was originally motivated by the apparent logarithmic behaviour of the potential in the region sensitive to the data. The optimum fit is shown in Table 3 and corresponds to the parameter values

$$A = -6.00, \quad B = 5.78, \quad v = 0.118$$
$$m_c = 1.43, \quad m_b = 4.83 \tag{4.5}$$

in GeV units. This is a purely phenomenological potential and cannot be compared to the short-distance perturbative potential. We see that it does not achieve a satisfactory description of all the $b\bar{b}$ data.

(ii) Richardson Potential [29]. Richardson proposed an economical potential which depends on a single parameter Λ_R

$$\tilde{V}(\mathbf{q}^2) = -\frac{4}{3}\frac{12\pi}{33-2n_f}\frac{1}{\mathbf{q}^2}\frac{1}{\ln(1+\mathbf{q}^2/\Lambda_R^2)}. \tag{4.6}$$

With this form we obtain the excellent fit to the data, shown in Table 2, for the parameter values

$$\Lambda_R = 0.375 \text{ GeV}, \quad m_c = 1.50 \text{ GeV}, \quad m_b = 4.91 \text{ GeV}. \tag{4.7}$$

However the potential is not constructed to reproduce the two-loop perturbative form and hence the parameter Λ_R has little to do with the perturbative QCD scale parameter $\Lambda = \Lambda^{(4)}_{\overline{\text{MS}}}$ which we are trying to measure. Indeed the value of Λ_R is determined from the data by the intermediate and long-range behaviour of the potential and not by its short distance behaviour. However it is worth noting that this one-parameter potential form gives an exceptionally good fit to the $c\bar{c}$ and $b\bar{b}$ data (see Table 3).

(iii) Kühn-Ono Potential [3]. A potential based on the second-order perturbative form in the massless 4-flavour effective theory was considered in [3];

$$V(r) = -\frac{16\pi}{25}\frac{1}{rf(r)}\left[1 + \frac{2\gamma_E + 53/75}{f(r)} - \frac{462\ln f(r)}{625 f(r)}\right] + a\sqrt{r} + c \tag{4.8a}$$

with

$$f(r) \equiv \ln[1/(\Lambda r)^2 + b], \tag{4.8b}$$

where the parameter b is introduced to avoid the Landau singularity. Here $\Lambda = \Lambda^{(4)}_{\overline{\text{MS}}}$ is the same QCD scale parameter as ours apart from the fact that they set $m_c = 0$. As discussed in Sect. 2, this causes a downward shift of about 20 MeV in the value of Λ when fitted

Table 3. The optimum fits to the quarkonia data using various potential forms. The masses are given in MeV and the leptonic widths, $\Gamma_n \equiv \Gamma_{ee}(nS)$, in keV. The data marked by ⋆ are not included in the fits

		Martin		Richardson		Kühn-Ono, $\Lambda=0.2$		Kühn-Ono, $\Lambda=0.4$	
$c\bar{c}$ data:			χ^2		χ^2		χ^2		χ^2
$m(1S)$	3068 ± 2	3068	0	3068	0	3068	0	3068	0
$m(2S)-m(1S)$⋆	595 ± 2	615	–	588	–	596	–	593	–
$m(1P)-m(1S)$	457 ± 10	441	1.4	423	11.5	429	7.7	427	9.1
Γ_2/Γ_1	0.43 ± 0.06	0.39	0.5	0.44	0.0	0.42	0.1	0.42	0.0
Γ_1⋆	4.75 ± 0.51	4.34	–	4.63	–	3.65	–	3.94	–
$b\bar{b}$ data:									
$m(1S)$	9452 ± 2.5	9452	0	9452	0	9452	0	9452	0
$m(2S)-m(1S)$	567 ± 3	575	7.6	569	0.6	572	2.9	570	0.8
$m(3S)-m(1S)$	900 ± 2.5	913	28.2	899	0.0	901	0.3	901	0.2
$m(1P)-m(1S)$	448 ± 2.5	413	190.0	451	2.1	444	2.9	446	0.6
$m(2P)-m(1S)$	809 ± 6	800	2.3	805	0.4	804	0.7	806	0.3
Γ_2/Γ_1	0.44 ± 0.03	0.50	4.4	0.41	1.1	0.43	0.2	0.42	0.2
Γ_3/Γ_1	0.33 ± 0.03	0.34	0.1	0.28	2.2	0.29	1.7	0.29	1.7
Γ_1⋆	1.22 ± 0.05	0.69	–	1.32	–	1.12	–	1.22	–
χ^2_{data}			235		17.9		16.4		13.0
$\chi^2_{\tilde{\nu}}$			–		–		25.9		22.4

Table 4. The parameter values corresponding to the fits shown in Table 2 for the Kühn-Ono potential form of (4.8)

Λ (GeV)	a $(\text{GeV})^{\frac{3}{2}}$	b	c (GeV)	m_c (GeV)	m_b (GeV)
0.2	0.67	238	−0.41	1.22	4.66
0.4	0.70	499	−0.81	1.41	4.83

to the same data. The optimum fit to the data using the potential of (4.8a) is shown in Table 3 for $\Lambda=0.2$ and for $\Lambda=0.4$ GeV, and the corresponding parameter values are given in Table 4. Excellent descriptions are obtained provided the regularization parameter b is allowed to take arbitrary values.⋆ The approach of the Kühn-Ono potential to the perturbative potential at short distances is relatively slow due to the large value of the regularization parameter b and also to the presence of the constant term, c, in the potential. The $\chi^2_{\tilde{\nu}}$ values are shown in Table 3 and , though large, are acceptable. However as Λ is decreased below 0.15 GeV the value of $\chi^2_{\tilde{\nu}}$ increases rapidly, as in Fig. 7, confirming once again that the $c\bar{c}$ and $b\bar{b}$ data cannot accommodate a short-distance potential with $\Lambda \lesssim 0.15$ GeV.

All the above potentials are compared in Fig. 8. As expected, they have a common slope in the region

⋆ With $b=20$, as taken in [3], we find $\chi^2_{\text{data}}=84.3$ for $\Lambda=0.2$ GeV and $\chi^2_{\text{data}}=630$ for $\Lambda=0.4$ GeV

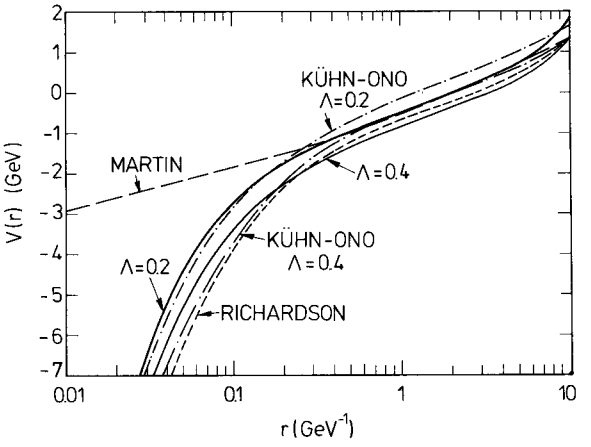

Fig. 8. Quarkonia potentials, obtained by fitting various phenomenological forms [given by (4.4), (4.6) and (4.8)] to the $c\bar{c}$ and $b\bar{b}$ data of Table 1, compared with the potential of (3.2) for two representative Λ values

sensitive to the $c\bar{c}$ and $b\bar{b}$ data, $0.5 < r < 5$ GeV^{-1}. At short distances both our potential and the Kühn-Ono potential behave roughly as the two-loop perturbative potential. The Richardson potential with $\Lambda_R = 0.375$ GeV gives the most singular behaviour at short distances, but is not too different from the two-loop behaviour with $\Lambda^{(4)}_{\overline{\text{MS}}}=0.5$ GeV around $r=0.1$ GeV^{-1}. At large distances ($r \gtrsim 5$ GeV^{-1}), the linearly rising behaviour of our potential and that of Richardson is clearly seen.

5. Predictions for Toponium as a Function of Λ

Our main objective is to see with what accuracy the value of $\Lambda \equiv \Lambda^{(4)}_{\overline{\rm MS}}$ can be determined by toponium data when it becomes available. The toponium spectrum is expected to be much richer than either of those of charmonium and bottomonium. The number of narrow toponium S states below the threshold for pair-production of $T(t\bar{q})$ mesons is predicted to be [38, 5]

$$n \simeq 3.8 \left(\frac{m_t}{m_b}\right)^{\frac{4}{3}}.$$

Taking $m_t = 40$ GeV we anticipate about 10 narrow toponium S states.

The predictions for the S states of the toponium spectrum are shown in Table 5 for the quarkonium potentials with $\Lambda = 0.2$ and $\Lambda = 0.4$ GeV obtained in the fit to the $c\bar{c}$ and $b\bar{b}$ data of Table 1. For comparison we also show the predictions of the "Martin" and "Richardson" potentials of (4.4) and (4.6) respectively. We see that the level spacings of the higher radial excitations ($n \geqq 3$) has little dependence on the choice of potential since they are sensitive to the region of the potential constrained by the $c\bar{c}$ and $b\bar{b}$ data. The observation of these higher excited states is still important in order to test the flavour independence of the potential. However, the decreasing separation between the higher excited states will make the states much more difficult to resolve experimentally [5, 39].

Table 5. Predictions for the toponium S states obtained using potentials that describe $c\bar{c}$ and $b\bar{b}$ data. We have taken $m(1S) = 80$ GeV

n	$\langle r^2 \rangle^{\frac{1}{2}}_{nS}$ $(\text{GeV})^{-1}$	$E_{n+1} - E_n$ in MeV			
		$\Lambda = 0.2$	$\Lambda = 0.4$	Richardson	Martin
1	0.35	670	746	987	505
2	0.82	358	363	372	298
3	1.32	224	221	228	215
4	1.89	157	161	170	170
5	2.43	130	135	140	141
6	2.88	118	121	120	121
7	3.23	111	111	108	106
8	3.71	105	104	98	95
9	3.88	100	98	91	85
10	4.16				

Fortunately the $1S$, $2S$ and (provided the toponium mass is less than about 80 GeV) also the $1P$ level are the states for which quantitative measurements are possible [5]. These toponium levels exhibit a strong Λ dependence as shown in Table 6. The predictions for five different values of $\Lambda = \Lambda^{(4)}_{\overline{\rm MS}}$ are shown for three possible toponium masses, $m(1S) = 60$, 80 and 100 GeV, and are obtained by minimizing $\chi^2_{\rm data} + \chi^2_V$ by fitting the quarkonium potential to the $c\bar{c}$ and $b\bar{b}$ data as well as to its perturbative short-distance form, as explained in Sect. 3. In Table 6 and in the following, $\Gamma^{(0)}_n$ stands for the 'virtual-photon contribution' to the leptonic width of the triplet nS states,

$$\Gamma^{(0)}_n = \Gamma(nS \to \gamma^* \to e^+ e^-) \tag{5.1}$$

including the first-order QCD correction, that is $\Gamma^{(0)}_n$ is used to denote $\Gamma_{ee}(nS)$ of (4.2). The true leptonic width, including the effects of the Z-boson contribu-

Table 6. Predictions for the properties of toponium that are most sensitive to the value of $\Lambda = \Lambda^{(4)}_{\overline{\rm MS}}$, shown for various values of the toponium mass, $m(1S)$, and various values of Λ. The potential is obtained by fitting to the $c\bar{c}$ and $b\bar{b}$ data as in Table 1

$m(1S)$ (GeV)	Λ (GeV)	Mass differences in MeV				$\Gamma^{(0)}_1$ (keV)	$\frac{\Gamma^{(0)}_2}{\Gamma^{(0)}_1}$	$\frac{\Gamma^{(0)}_3}{\Gamma^{(0)}_1}$
		$2S-1S$	$3S-1S$	$1P-1S$	$2P-1S$			
60	0.1	603	945	458	853	2.58	0.53	0.32
	0.2	652	997	517	913	3.35	0.46	0.27
	0.3	679	1025	550	945	3.82	0.43	0.24
	0.4	707	1051	582	975	4.26	0.40	0.22
	0.5	752	1090	627	1017	4.73	0.37	0.20
80	0.1	603	954	473	863	2.65	0.50	0.32
	0.2	670	1028	548	945	3.54	0.42	0.26
	0.3	708	1069	590	990	4.09	0.40	0.23
	0.4	746	1108	630	1033	4.60	0.37	0.21
	0.5	802	1162	681	1090	5.08	0.35	0.19
100	0.1	610	964	492	877	2.79	0.46	0.30
	0.2	694	1059	583	978	3.78	0.39	0.24
	0.3	741	1112	633	1034	4.40	0.36	0.22
	0.4	787	1163	680	1088	4.96	0.34	0.20
	0.5	851	1229	735	1158	5.45	0.34	0.18

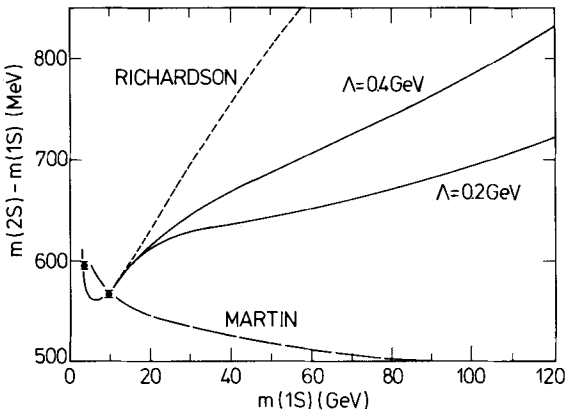

Fig. 9. The prediction of the $2S-1S$ mass difference for $\Lambda=0.2$ and 0.4 GeV (solid lines), compared to that of the Martin and Richardson potentials as a function of the toponium mass. The $\psi'-J/\psi$ and $\Upsilon'-\Upsilon$ mass differences are also shown. The former has not been used in the fit

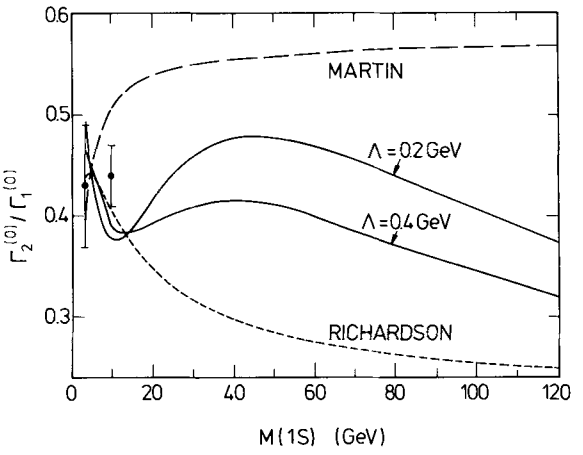

Fig. 11. The ratio of the toponium $2S$ to $1S$ leptonic widths as a function of the toponium mass; the ratio is expected to be essentially free from uncertainties due to QCD corrections. The ratios obtained from $c\bar{c}$ and $b\bar{b}$ data are also shown

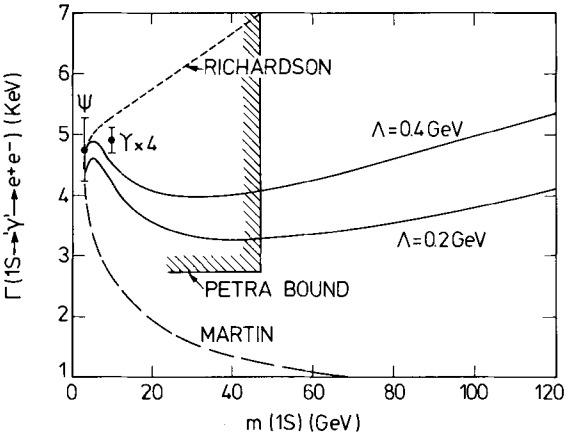

Fig. 10. The leptonic width $\Gamma(\theta\to"\gamma"\to e^+e^-)$ as a function of the toponium (θ) mass. Γ_{ee} is given by (4.2); the contribution of the virtual Z is omitted. The observed ψ and Υ leptonic widths are also shown, the latter multiplied by 4. These data have not been used in the fits

tion, is then trivially obtained from $\Gamma_n^{(0)}$ once the Z-boson mass and couplings are accurately measured [5]. From Table 6 we see, as Λ grows from 0.1 to 0.5 GeV, that both the $2S-1S$ and $1P-1S$ mass differences increase, and that $\Gamma_1^{(0)}$ grows, whereas the ratios $\Gamma_2^{(0)}/\Gamma_1^{(0)}$ and $\Gamma_3^{(0)}/\Gamma_1^{(0)}$ decrease.

In Figs. 9–11 we show the predictions for $m(2S)-m(1S)$, $\Gamma_1^{(0)}$ and $\Gamma_2^{(0)}/\Gamma_1^{(0)}$ respectively, over a wide range of $m(1S)$ values, that are obtained from our potential with $\Lambda=0.2$ and 0.4 GeV, together with those we have obtained using a Richardson-type potential and a Martin-type potential. It should be noted that the $\psi'-J/\psi$ mass difference shown in Fig. 9 and the J/ψ and Υ leptonic width data shown in Fig. 10 were not included in the fits as explained in Sect. 4. Nevertheless, all the potentials give satisfactory descriptions of the $c\bar{c}$ and $b\bar{b}$ data with the exception of the large discrepancy in the Υ leptonic width predicted by the Martin-type potential (see Fig. 10).

For high mass quarkonium states we see from the figures that the predictions of the different potentials models are very clearly distinguished. The Richardson potential predicts a rapid growth of the $2S-1S$ mass difference and of the leptonic width with increasing quarkonium mass, whereas the Martin potential products a decrease of these quantities. The potentials whose short-distance behaviour is controlled by two-loop perturbative QCD give intermediate predictions, reflecting a milder short-distance behaviour as compared to that of Richardson's potential but more singular than the Martin form (see Fig. 8).

Note that the curves shown in Fig. 10 for the leptonic widths included the first-order QCD correction factor of $(1-16\alpha_s/3\pi)$ in (4.2). This large correction (about 30% for $\Gamma_{ee}(\Upsilon)$) means the leptonic width predictions are unreliable. For instance, by simply replacing the correction factor by the positive-definite form $(1+16\alpha_s/3\pi)^{-1}$ makes the $\Lambda=0.4$ GeV prediction for $\Gamma_1^{(0)}$ agree with the $\Upsilon\to e^+e^-$ data (see Fig. 10). Such ambiguities in $\Gamma_1^{(0)}$ are largely cancelled in the ratio of branching fractions shown in Fig. 11 and so Γ_2/Γ_1 rather than Γ_1 should be used to probe the short-distance part of the potential and to determine Λ.

Finally, we study the extent to which the prospective toponium measurements will be able to determine the QCD parameter Λ. For this purpose we assume a toponium mass of $m(1S)=80$ GeV and include in the fit 'dummy' toponium data which could be obtained at the forthcoming e^+e^- colliders. To be pre-

cise the toponium 'data' are taken to be the values predicted by our potential but with statistical errors corresponding to those expected to be achieved at LEP, as estimated by the LEP study group [5]. We show results for two sets of toponium 'data', namely those with central values predicted by our $\Lambda=0.2$ and $\Lambda=0.4$ GeV potentials given in Table 1. For $\Lambda=0.2$ GeV we have

$$m(2S)-m(1S)=670\pm 20 \text{ MeV}, \tag{5.2a}$$

$$\Gamma_2^{(0)}/\Gamma_1^{(0)}=0.42\pm 0.06 \tag{5.2b}$$

and for $\Lambda=0.4$ GeV

$$m(2S)-m(1S)=746\pm 20 \text{ MeV}, \tag{5.3a}$$

$$\Gamma_2^{(0)}/\Gamma_1^{(0)}=0.37\pm 0.06. \tag{5.3b}$$

Here we have taken a 20 MeV error on the mass difference and a 15% error on the ratio of the leptonic widths as anticipated [5] to be relevant to the forthcoming experiments. We include the toponium 'data' with the $c\bar{c}$ and $b\bar{b}$ data listed in Table 1 and perform a fit to the combined data as a function of Λ as explained in Sect. 4. The top quark mass is determined by requiring $m(1S)=80$ GeV. The results of the χ^2 fits are shown by the dashed curves in Fig. 12 superimposed on the χ^2 curve of Fig. 7a which corresponds to the fit to the $c\bar{c}$ and $b\bar{b}$ data alone. If one allows χ^2 values up to $\chi^2_{\min}+3$ then we see that toponium data should be able to determine $\Lambda\equiv\Lambda^{(4)}_{\overline{\text{MS}}}$ to an accuracy of just less than ± 100 MeV.

We find that it is essentially the mass difference 'data' which determines Λ. The 'data' of (5.2b) (or (5.3b)) for the ratio of the leptonic widths gives only a weak constraint on the value of Λ. These conclusions can be anticipated from Figs. 9 and 11. From Fig. 10 we see that the width $\Gamma_1^{(0)}$ is more sensitive to Λ than the ratio $\Gamma_2^{(0)}/\Gamma_1^{(0)}$. Indeed if 'data' for $\Gamma_1^{(0)}$ with the expected accuracy [5] of 10% is incorporated into the fit, and if prediction (4.2) for $\Gamma_1^{(0)}$ is taken at face value, then the χ^2 versus Λ profile is shown by the dotted curve in Fig. 12 and we see Λ is determined to within ± 85 MeV. However from (4.2) we note that the first-order QCD corrections to the leptonic width are $-16\alpha_s/3\pi$ relative to unity and so we expect higher-order corrections of order $(16\alpha_s/3\pi)^2$, that is of the order of about 5%. It is clearly important to reduce the theoretical uncertainty in (4.2) so that the measurement of $\Gamma_1^{(0)}$ can be reliably incorporated into the fit and hence the determination of Λ can be improved.

We also studied the possible improvement in the determination of Λ if the $1P$ toponium state was observed, for example via $2S\to 1P\gamma\to 1S\gamma\gamma$. Including a measurement of the $1P-1S$ mass difference with an error ± 20 MeV in the fit results in a χ^2 versus

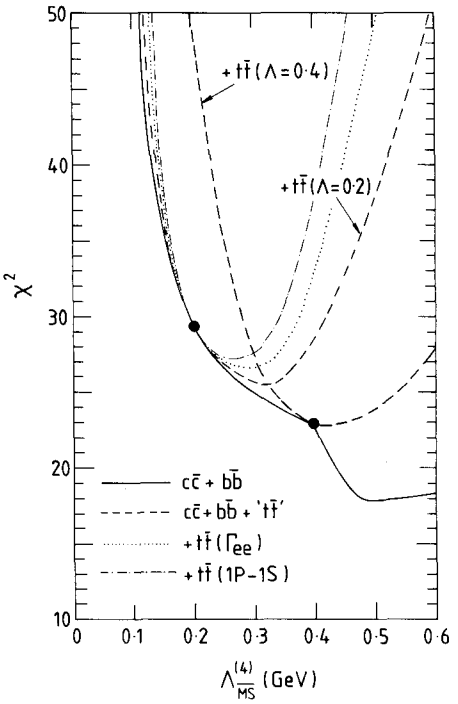

Fig. 12. The effect of including toponium 'data' in the fit to determine Λ. The continuous curve is the χ^2 profile obtained by fitting to $c\bar{c}$ and $b\bar{b}$ as presented in Fig. 7a. The dashed curves show the effect of including the toponium 'data' of either (5.2) or (5.3). These 'data' are the predictions of our $\Lambda=0.2$ and 0.4 potentials respectively and so give zero additional χ^2 contributions at these values (as indicated by the solid dots). The dotted curve shows the effect of including $\Gamma_1^{(0)}=3.54\pm 0.35$ keV in the fit rather than the ratio of (5.2b). The dot-dashed curve shows the improvement obtained by including, in addition, the $1P-1S$ mass difference of 548 ± 20 MeV

Λ profile shown by the dot-dashed curve in Fig. 12, leading to a determination of Λ to within about ± 75 MeV.

We studied the sensitivity of our conclusions to omitting the $c\bar{c}$ data from the fits. We found very similar results, thereby decreasing the sensitivity of the analysis to relativistic corrections.

We also checked to see whether the determination of Λ is biased by the parametric form used for the potential. First we fitted the $c\bar{c}$, $b\bar{b}$ and '$t\bar{t}$' data by adding one more parameter in the intermediate potential

$$V_I(r)=r(c_1+c_2r+c_3r^2)\exp(-r/r_0).$$

The χ^2 curves as a function of Λ are essentially the same as those shown in Fig. 12. Next, we studied the effect of including a constant term V_0 in the potential. We repeated the combined fit to the $c\bar{c}$, $b\bar{b}$ and '$t\bar{t}$' shown in Fig. 12 for $V_0=0$ but now leaving V_0 as a free parameter and we found very similar χ^2 profiles with minima at the same values of Λ. We conclude

the determination of Λ does not depend on whether V_0 is included or set equal to zero.

6. Conclusions

We have critically re-examined the sensitivity of the charmonium and bottomonium data to the short-distance part of the interquark potential in the framework of the non-relativistic quark model. We studied the next-to-leading order QCD perturbative prediction for the potential and quantitatively investigated both its region of validity and the effects of heavy quark loops. By using a phenomenological potential which embodies the short-distance perturbative behaviour and long-distance linear confinement and which has a flexible form for intermediate distances, we find that the $c\bar{c}$ and $b\bar{b}$ data do not constrain the QCD scale parameter $\Lambda \equiv \Lambda^{(4)}_{\overline{\rm MS}}$ apart from requiring $\Lambda \gtrsim 150$ MeV.

Predictions for the properties of higher mass quarkonium states are found to be quite sensitive to the value of Λ, confirming previous observations (see, for example, [1, 2]). When compared to the predictions of other potentials, two extremes being the Richardson- [29] and the Martin- [30] type potential, the predictions of the potentials which incorporate the next-to-leading order perturbative behaviour are distinctively different for $m(2S)-m(1S)$ and $\Gamma(2S\to e^+e^-)/\Gamma(1S\to e^+e^-)$ which are expected to be measured rather accurately for toponium at LEP [5]. An important question is how well the toponium measurements will be able to determine Λ. We investigated this question by assuming sample 'data' for the above two quantities around the predictions of our potential and with statistical errors expected in the forthcoming experiments. By performing a χ^2 fit as a function of Λ to the toponium 'data' together with the $c\bar{c}$ and $b\bar{b}$ data we concluded that the toponium measurements could only determine Λ to within ± 100 MeV if Λ is the region 0.2–0.5 GeV.

With the anticipated experimental errors [5] we find that Λ is essentially determined by the $2S-1S$ toponium mass difference and that the ratio of the leptonic widths is rather insensitive to Λ. It is fortunate that the $2S-1S$ mass difference is the quantity most sensitive to Λ as it is also the quantity most accessible to accurate experimental determination. We took the error on the measurement of the mass difference to be 20 MeV corresponding to that expected* for toponium of mass 80 GeV. If the toponium mass turns out to be either 70 or 90 GeV then the $2S-1S$ mass difference can be measured more accurately, with errors* of 10 and 15 MeV respectively, and consequently a more precise determination of Λ can be achieved. The absolute measurement of the mass may have a systematic error of about 100 MeV but fortunately this is not relevant to the measurement of the mass difference.

Although the ratio of the leptonic widths do not put much constraint on the value of Λ, the situation can be improved by including the width $\Gamma(1S\to e^+e^-)$ in the fit. The width is expected to be measured to 10% accuracy, and including such a measurement in the analysis would determine Λ to within about ± 85 MeV. However we would first have to compute the higher order QCD corrections to the formula for $\Gamma(1S\to e^+e^-)$ to ensure the theoretical prediction is sufficiently reliable.

* The expected experimental accuracy assumes a luminosity of 0.4 pb^{-1} at nine different energies in the resonance region, see [5]

Acknowledgements. One of us (KH) thanks S. Jacobs, K.J. Miller and M.G. Olsson for an earlier collaboration. We thank S. Jacobs for information and A. Kronfeld and M. Lüscher for discussions. AWP thanks the UK Science and Engineering Research Council for the award of a Research Studentship.

References

1. W. Buchmüller, S.-H.H. Tye: Phys. Rev. **D24**, 132 (1981); W. Buchmüller, G. Grunberg, S.-H.H. Tye: Phys. Rev. Lett. **45**, 103, 587(E) (1980)
2. K. Hagiwara, S. Jacobs, M.G. Olsson, K.J. Miller: Phys. Lett. **130B**, 209 (1983)
3. J.H. Kühn, S. Ono: Z. Phys. C – Particles and Fields **21**, 395 (1984); C – Particles and Fields **24**, 404(E) (1984)
4. P. Moxhay, J.L. Rosner: Phys. Rev. **D28**, 1132 (1983)
5. W. Buchmüller et al.: Physics at LEP, CERN 86-02, Vol. 1, p. 203 (1986)
6. S. Schmitz, D. Beavis, P. Kaus: University of California – Riverside preprint, UCR-TH-85-3 (1985)
7. K. Igi, S. Ono: Phys. Rev. **D33**, 3349 (1986)
8. L. Susskind: in Weak and electromagnetic interactions at high energy , Les Houches 1976, p. 207. Amsterdam: North Holland 1977
9. D.J. Gross, F. Wilczek: Phys. Rev. Letts. **30**, 1343 (1973); H.D. Politzer: Phys. Rev. Lett. **30**, 1346 (1973)
10. T. Appelquist, M. Dine, I.J. Muzinich: Phys. Lett. **69B**, 231 (1977); F. Feinberg: Phys. Rev. Lett. **39**, 316 (1977); W. Fischer: Nucl. Phys. **B129**, 157 (1977)
11. A. Billoire: Phys. Lett. **92B**, 343 (1980)
12. W.A. Bardeen, A.J. Buras, D.W. Duke, T. Muta: Phys. Rev. **D18**, 3998 (1978)
13. D.W. Duke, R.G. Roberts: Phys. Rep. **120**, 275 (1985)
14. K. Hagiwara: Supp. Prog. Theor. Phys. **77**, 101 (1983)
15. G. 't Hooft: Nucl. Phys. **B72**, 461 (1974)
16. G. Grunberg: Phys. Lett. **95B**, 70 (1980); Phys. Lett. **114B**, 271 (1982); Phys. Rev. **D29**, 2315 (1984)
17. O.U. Tarasov, A.A. Valdimirov, A.Yu. Zharkov: Phys. Lett. **93B**, 429 (1980)
18. E. Braaten, J.P. Leveille: Phys. Rev. **D24**, 1369 (1981)
19. K. Hagiwara and T. Yoshino: Phys. Rev. **D26**, 2038 (1982)
20. K. Hagiwara: Phys. Lett. **118B**, 141 (1982)
21. T. Kinoshita: J. Math. Phys. **3**, 650 (1962); T.D. Lee, M. Nauenberg: Phys. Rev. **133**, B1549 (1964)
22. K. Symanzik: Commun. Math. Phys. **34**, 7 (1973); T. Appelquist, J. Carazzone: Phys. Rev. **D11**, 2856 (1975)

23. S. Weinberg: Phys. Lett. **91B**, 51 (1980); B. Ovrut, H.J. Schnitzer: Phys. Rev. **D21**, 3369 (1980)
24. S. Weinberg: in [23]; L. Hall: Nucl. Phys. **B178**, 75 (1981); W. Bernreuther, W. Wetzel: Nucl. Phys. **B197**, 228 (1982); W.J. Marciano: Phys. Rev. **D29** 580 (1984)
25. W. Kummer: Phys. Lett, **105B** 473 (1981)
26. T. Yoshino, K. Hagiwara: Z. Phys. C – Particles and Fields **C24**, 185 (1984)
27. W. Celmaster, R.J. Gonsalves: Phys. Rev. **D20**, 1420 (1979)
28. J.H. Kühn: Acta Phys. Polon. **B12**, 347 (1981)
29. J.L. Richardson: Phys. Lett. **82B**, 272 (1979)
30. A. Martin: Phys. Lett. **93B**, 338 (1980)
31. C. Bachas: Phys.Rev. **D33**, 2723 (1986)
32. Particle Data Group: Phys. Lett. **170B**, 1 (1986)
33. A.D. Steiger: Phys. Lett. **129B**, 335 (1983)
34. W. Celmaster: Phys. Rev. **D19**, 1517 (1979)
35. K.J. Miller, M.G. Olsson: Phys. Rev. **D25**, 2383 (1982)
36. E. Eichten et al.: Phys. Rev. **D17**, 3090 (1978)
37. C. Quigg, J.L. Rosner: Phys. Lett. **72B**, 462 (1978)
38. C. Quigg, J.L. Rosner: Phys. Rep. **56**, 167 (1979)
39. A.D. Martin: Proc. New Particles '85 Conf., Madison, p. 24, ed. V. Barger, D. Cline, F. Halzen. Singapore: World Scientific 1986)